WAVES IN THE SUNSPOT UMBRA

H. M. ANTIA and S. M. CHITRE
Tata Institute of Fundamental Research, Homi Bhabha Road, Bombay 400 005, India

(Received 30 November, 1978)

Abstract. The magnetoacoustic modes excited in a thermally conducting polytropic fluid layer in the presence of a vertical magnetic field are examined with a view to classify them with the help of phase diagrams. The possibility of identifying the umbral flashes with overstable magnetoacoustic modes is explored.

1. Introduction

The generation and propagation of hydromagnetic waves in the solar atmosphere have received considerable attention because of their possible role in providing the necessary energy to heat the overlying layers and also because of their importance in accounting for some of the features associated with active regions. Specifically, there have been observations in sunspots of flashes in the umbra and running penumbral waves (Giovanelli, 1972). Suggestions have been made by Savage (1969), Moore (1973), and more recently by Uchida and Sakurai (1975) that overstable oscillatory motion is a possible mechanism to account for both these phenomena. Furthermore the overstable oscillations are also important from the theoretical point of view, since the theoretical work of Chitre (1963) and Deinzer (1965) necessarily requires some mode of non-radiative energy transport in order to produce consistent spot models. Parker (1974) has suggested that Alfvén waves can account for the 'missing energy' of sunspots. However Parker's work has been criticised by Cowling (1976), pointing out that the incompressibility assumption and the Boussinesq approximation do not permit any distinction between Alfvén waves and magnetoacoustic waves; the motions excited by overstability are expected to be quite different from those corresponding to Alfvén waves.

The umbral flashes which appear as periodic brightening in sunspots were first observed in the H and K lines and also in Hα lines (Zirin and Stein, 1972). The flashes manifest themselves as bright spots of approximately 1000 km in diameter occurring in coherent sequences with a period ranging from 110 s to 190 s. Although flashing may appear continuously for several hours in the umbra, a coherent sequence normally lasts only up to an hour or so. It is also observed that the flashes which seem to arise in the central regions of the umbra move out towards the penumbra with an average speed of 40 km s^{-1}. In large sunspots along with umbral flashes the running penumbral waves are seen and there is some evidence that the two are phase locked. There is some indication that the larger the spot magnetic field, the shorter is the period associated with umbral flashes and penumbral waves.

It is well known that sunspots are endowed with strong magnetic fields (≥ 2000 G) and the field is largely vertical in the umbral region. The stability of a fluid layer in the

Solar Physics **63** (1979) 67–78. 0038–0938/79/0631–0067 $01.80.

presence of a vertical magnetic field has been discussed by Chandrasekhar (1961) and more recently by Savage (1969) and Parker (1974). But all these investigations are performed in the framework of the Boussinesq approximation which ignores the effects of compressibility and the consequent density variation in the steady state. Such an analysis is hardly applicable to sunspots where there is believed to be a substantial density variation from the base of the spot to its surface. Besides, the fast (magnetoacoustic) modes are filtered out in the Boussinesq approximation and it is just these modes which turn out to be very important in understanding the velocity fields in the sunspot penumbra (Nye and Thomas, 1976; Antia *et al.*, 1978, hereafter referred to as Paper I). The effect of compressibility has been considered by McLellan and Winterberg (1968), Bel and Mein (1971), and more recently by Bel and Leroy (1977). These authors have studied the local dispertion relation and thus although their analysis includes the fast modes, still it does not incorporate density variation in the steady state. Furthermore they have not considered the effect of thermal dissipation, without which the oscillatory modes are always neutral.

The motivation of the present work is to include the full effects of compressibility and thermal dissipation on the modes excited in a fluid layer in the presence of a vertical magnetic field. For the sake of simplicity we study the stability of a thermally conducting polytropic fluid layer with infinite electrical conductivity, pervaded by a uniform vertical magnetic field. We explore the possibility of identifying the umbral flashes with overstable magnetoacoustic modes excited in such a fluid layer.

The rest of the paper is arranged as follows: the basic equations and boundary conditions are set out in Section 2, the classification of oscillatory modes into fast and slow modes is considered in Section 3. Finally the numerical results and discussion are given in Section 4.

2. Mathematical Formulation

We investigate the linear stability of a plane parallel thermally conducting inviscid fluid layer stratified under constant gravity in the presence of a uniform vertical magnetic field. Further we assume the fluid to be an ideally conducting perfect gas with unit magnetic permeability. The governing equations in the usual notation are:

$$\rho\left(\frac{\partial \mathbf{v}}{\partial t}+(\mathbf{v}\cdot\nabla)\mathbf{v}\right)=-\nabla p+\rho\mathbf{g}+\frac{\mathbf{j}\times\mathbf{B}}{c}, \qquad \frac{\partial\rho}{\partial t}+\nabla\cdot(\rho\mathbf{v})=0,$$

$$\rho C_v\left(\frac{\partial T}{\partial t}+\mathbf{v}\cdot\nabla T\right)-RT\left(\frac{\partial\rho}{\partial t}+\mathbf{v}\cdot\nabla\rho\right)=\nabla\cdot(K\nabla T), \qquad P=R\rho T,$$

$$\nabla\times\mathbf{H}=\frac{4\pi}{c}\mathbf{j}, \qquad \nabla\times\mathbf{E}=-\frac{1}{c}\frac{\partial\mathbf{B}}{\partial t},$$

$$\nabla\cdot\mathbf{B}=0, \qquad \mathbf{E}+\frac{\mathbf{v}\times\mathbf{B}}{c}=0.$$

Assuming the static state to be polytropic with the associated index $\Gamma = (\mathrm{d} \ln P_0)/(\mathrm{d} \ln \rho_0)$, and following the same procedure and approximations as given in Paper I we arrive at the following set of perturbed equations in the dimensionless form with distance expressed in units of RT_0/g and time in $\sqrt{RT_0/g}$. Hereafter all quantities are assumed to be in dimensionless form unless otherwise stated:

$$\frac{\mathrm{d}(\rho_0 v_z)}{\mathrm{d}z} = \frac{\omega \rho_0}{T_0}\theta - \frac{\omega}{T_0}P_1 - k_x \rho_0 (iv_x)\,,$$

$$\frac{\mathrm{d}P_1}{\mathrm{d}z} = -\omega(\rho_0 v_z) + \frac{\rho_0}{T_0}\theta - \frac{P_1}{T_0}\,,$$

$$G_k \frac{\mathrm{d}^2\theta}{\mathrm{d}z^2} = -\left[1 - \frac{\gamma}{\Gamma} + G_k \frac{(\lambda+1)\omega T_0'}{T_0 \rho_0}\right](\rho_0 v_z) - \omega(\gamma - 1)P_1 + \tag{1}$$

$$+ (G_k k_x^2 + \omega\gamma\rho_0)\theta + G_k \frac{(\lambda+1)}{T_0}\frac{\mathrm{d}\theta}{\mathrm{d}z}\,,$$

$$G_B \frac{\mathrm{d}^2(iv_x)}{\mathrm{d}z^2} = -\omega k_x P_1 + (G_B k_x^2 + \omega^2 \rho_0)(iv_x)\,.$$

Here P_1 and θ are the perturbations in the pressure and temperature respectively, v_x and v_z are the components of velocity $\mathbf{v}$ in x and z directions, γ is the ratio of specific heats, K_0 is the constant thermal conductivity in steady state. The opacity is assumed to be of the form $\sim T^{\nu}\rho^{\lambda}$, where the constants ν and λ are adjusted so as to make conductivity K_0 constant in steady state. In Equations (1)

$$G_k = \frac{K_0 g}{\rho_{\mathrm{base}} C_v (RT_{\mathrm{base}})^{3/2}} \quad \text{and} \quad G_B = \frac{B_0^2}{4\pi R T_{\mathrm{base}} \rho_{\mathrm{base}}}$$

are the dimensionless parameters which are measures of the effectiveness of radiative dissipation and magnetic field respectively. The quantities occurring on the right hand side of the definitions of G_B and G_k are in standard units.

It can be seen that this set of equations is of sixth order in z derivatives and hence for a complete specification of the problem we require in all six boundary conditions at the bounding surfaces. The four of these may be taken to be same as those for a non-magnetic fluid (viz. $v_z = 0$ and $\theta = 0$ at both the boundaries), while an additional boundary condition will have to be imposed on the magnetic flux perturbations at each of the boundaries. In the simplest cases this can be taken as $b_x = 0$ ($\mathrm{d}v_x/\mathrm{d}z = 0$) or $b_z = 0$ ($v_x = 0$), where b_x and b_z are respectively the horizontal and vertical components of magnetic field perturbations. Specifically we shall adopt the following three sets of boundary conditions.

(I) Fixed boundary conditions in which both the boundaries are maintained at constant temperature and there is no momentum flux across the boundaries. Further the perturbations in the horizontal component of magnetic field is also assumed to

vanish at both the boundaries, which gives

$$\rho_0 v_z = 0\,, \qquad \theta = 0 \quad \text{and} \quad \frac{\mathrm{d}v_x}{\mathrm{d}z} = 0 \quad \text{at} \quad z = 0 \quad \text{and} \quad z = d\,. \tag{2}$$

(II) Fixed boundary conditions in which the perturbation in the vertical component of magnetic field is assumed to vanish at both the boundaries, while the first two conditions are same as in the first case. This gives

$$\rho_0 v_z = 0\,, \qquad \theta = 0 \quad \text{and} \quad v_x = 0 \quad \text{at} \quad z = 0 \quad \text{and} \quad z = d\,. \tag{3}$$

(III) Free boundary conditions at the upper boundary, which demand the vanishing of the Lagrangian pressure perturbations and the horizontal component of magnetic field, and the linearization of the radiative flux condition. The lower boundary is assumed to be fixed as in (I):

$$\rho_0 v_z = 0\,, \qquad \theta = 0 \quad \text{and} \quad \frac{\mathrm{d}v_x}{\mathrm{d}z} = 0 \quad \text{at} \quad z = 0$$

and

$$\left.\begin{aligned} &\rho_0 v_z - \omega P_1 + k_x G_B (i v_x) = 0\,, \\ &\theta - \frac{\Gamma - 1}{\omega \Gamma} v_z + \frac{\Gamma T_0}{4(\Gamma - 1)} \frac{\mathrm{d}\theta}{\mathrm{d}z} = 0\,, \\ &\frac{\mathrm{d}v_x}{\mathrm{d}z} = 0\,, \end{aligned}\right\} \quad \text{at} \quad z = d\,. \tag{4}$$

The set of Equations (1) supplemented by the boundary conditions is solved numerically by a method described by Antia (1979) to obtain the complex eigenvalues ω and the corresponding eigenfunctions for various perturbed quantities. Most of the results are obtained for the first set of boundary conditions since for this case the eigenfunctions are simplest to handle and the classification of modes becomes relatively easy as will become evident in the following section.

3. Classification of Modes

We shall first discuss the classification of various modes that are excited in the compressible medium in the presence of a vertical magnetic field. It can be seen from Equations (1) that if $k_x = 0$, the last equation gets decoupled from the other equations; furthermore the remaining set of equations does not contain any term involving the magnetic field. This gives the usual acoustic modes for $k_x = 0$ (with $v_x \equiv 0$), while the last equation involving only v_x yields eigensolutions with $P_1 \equiv 0$, $v_z \equiv 0$ and $v_x \not\equiv 0$. These latter modes may be identified with the Alfvén waves with the wave-vector along the field lines. These Alfvén modes are not affected by thermal exchange and they remain neutral even in the presence of thermal dissipation. For small values of G_B, the Alfvén modes have lower frequency compared to the

corresponding acoustic modes. For $k_x = 0$ the frequency of Alfvén modes is proportional to $\sqrt{G_B}$ and consequently by increasing G_B sufficiently the frequencies can be made higher than those of acoustic modes which do not depend on G_B for the case $k_x = 0$. For non-zero values of k_x, the acoustic modes will have non-zero v_x and correspondingly the Alfvén modes will have non-zero v_z and P_1. For both the series of modes the number of nodes in various perturbed quantities increases with ω. As there is an overlap of the frequency of the two series, it is rather difficult to classify the modes, into two distinct series for moderate values of k_x. Because of the boundary conditions and stratification in the layer the various modes are a mixture of pure modes which we might have obtained for an infinite homogeneous medium, and hence there is no clear phase relationship between various perturbed quantities for the two series of modes. It is found that as k_x increases the frequency of the lower of the two series of modes (hereafter referred to as slow modes) decreases very gradually and should tend to a finite limit as $k_x \to \infty$. For small values of the magnetic field, some of these slow modes may become convective modes at higher values of k_x in the absence of thermal dissipation. However a sufficiently strong thermal dissipation restores their oscillatory character. On the other hand, the frequency of the higher of the two series of modes (hereafter referred to as fast modes) increases monotonically with k_x and tends to infinity as $k_x \to \infty$. Thus for very large values of k_x the fast modes have frequencies much higher than those of slow modes, and it is not difficult to distinguish between them. As the magnetic field decreases, the fast modes go over into the acoustic modes, while the slow modes go over into the gravity or convective modes depending on the temperature gradiant.

To classify the modes unambiguously into fast or slow modes we consider the non-dissipative case ($G_k = 0$). In this case the eigenvalues ω are purely imaginary for both the modes, and it is possible to eliminate θ from Equations (1) to get the following fourth order system of differential equations,

$$\begin{aligned}
\frac{\mathrm{d}}{\mathrm{d}z}\left(\frac{v_z}{\omega}\right) &= \frac{1}{\gamma T_0}\left(\frac{v_z}{\omega}\right) - \frac{1}{\gamma T_0 \rho_0} P_1 - \frac{ik_x}{\omega} v_x , \\
\frac{\mathrm{d}P_1}{\mathrm{d}z} &= \left[-\omega^2 + \frac{[1-(\gamma/\Gamma)]}{\gamma T_0} \right] \frac{\rho_0 v_z}{\omega} - \frac{1}{\gamma T_0} P_1 , \\
G_B \frac{\mathrm{d}^2 v_x}{\mathrm{d}z^2} &= i\omega k_x P_1 + (G_B k_x^2 + \omega^2 \rho_0) v_x .
\end{aligned} \tag{5}$$

To illustrate the classification of modes we shall consider the first set of boundary conditions which, for $G_k = 0$, become

$$v_z = 0 \quad \text{and} \quad \frac{\mathrm{d}v_x}{\mathrm{d}z} = 0 \quad \text{at} \quad z = 0 \quad \text{and} \quad z = d . \tag{6}$$

For these equations the eigenvalues are either real or purely imaginary. It is evident from the equations that for purely imaginary values of ω, the perturbed quantities v_z/ω, P_1 and v_x are all real and it is then possible to study their phase

relationship. It should be noted that the introduction of thermal dissipation produces only a small change in the eigenvalues making them complex, and the classification based on non-dissipative case serves as a good guide to the corresponding modes with dissipation. Further we appeal to the phase diagrams discussed extensively by Eckart (1960) and more recently by Scuflaire (1974) who has used it to classify the modes arising in the study of non-radial oscillations of condensed polytropes. However in the present case since the equation is of fourth order, both the slow and fast modes can have propagating (oscillatory) character simultaneously, above a certain frequency. To study the phase relations we plot all the six possible combinations of the four basic perturbed quantities $(v_z/\omega, P_1, v_x, \mathrm{d}v_x/\mathrm{d}z)$ against each other as shown in Figures 1 and 2, for different cases. For all the cases the plots are assumed to start from the base of the layer. It turns out that the various modes fall in two distinct classes (fast and slow) with the lowest fast mode (F0) occupying a unique position in the sense that it shares characteristics of both the classes of modes. The following features emerge from the plots which are displayed in Figures 1 and 2:

(1) $(v_x - P_1)$ and $[(\mathrm{d}v_x/\mathrm{d}z) - (v_z/\omega)]$ diagrams: These diagrams show the phase relation between v_x and P_1 and $\mathrm{d}v_x/\mathrm{d}z$ and v_z/ω. It is found that for lower values of G_B the eigenfunctions have some distinct phase relationship and can be clearly identified with the help of these diagrams. For fast modes v_x and P_1 (or, $\mathrm{d}v_x/\mathrm{d}z$ and

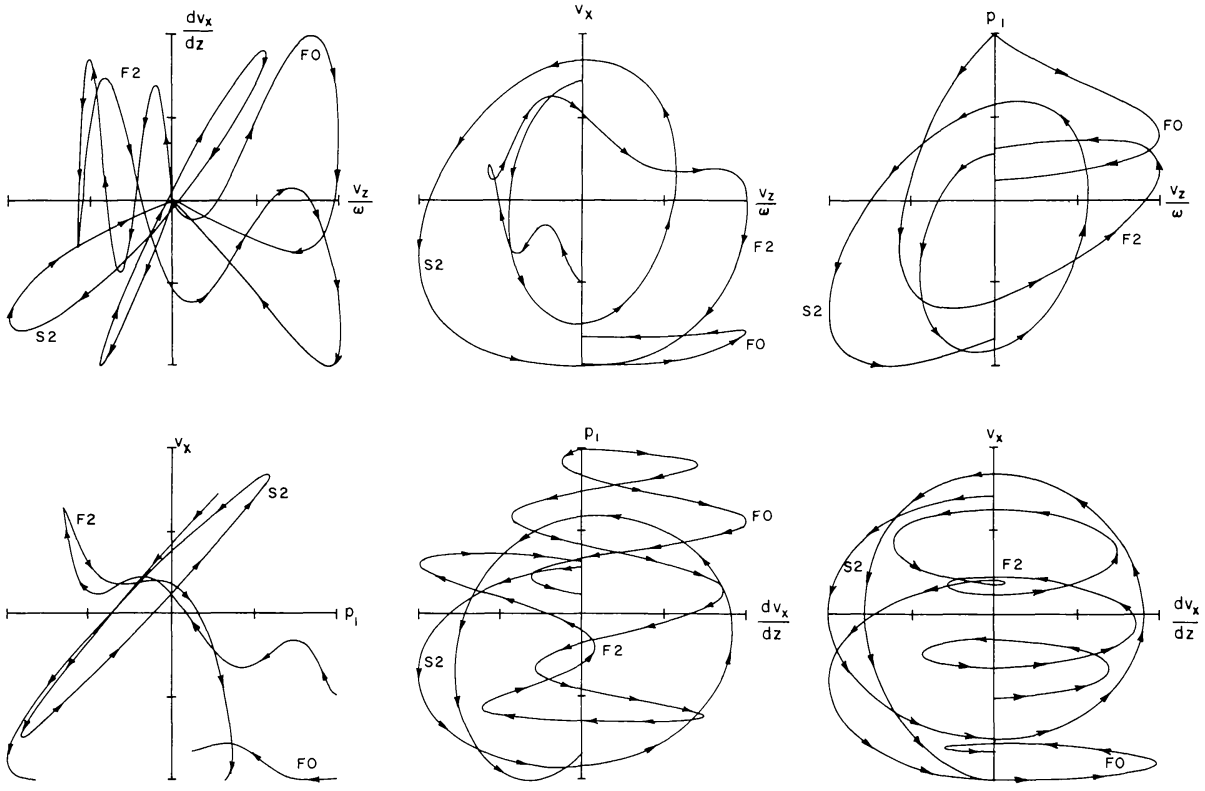

Fig. 1. The phase diagrams for $\Gamma = 1.66$, $G_B = 0.0239$, $T_r = 0.33$, $\gamma = 1.1$, and $k_x = 1.0$ displaying the relative phase of all six possible pairs of the four basic perturbed quantities $(v_z/\omega, P_1, v_x, \mathrm{d}v_x/\mathrm{d}z)$, for three different modes (F0, F2, and S2).

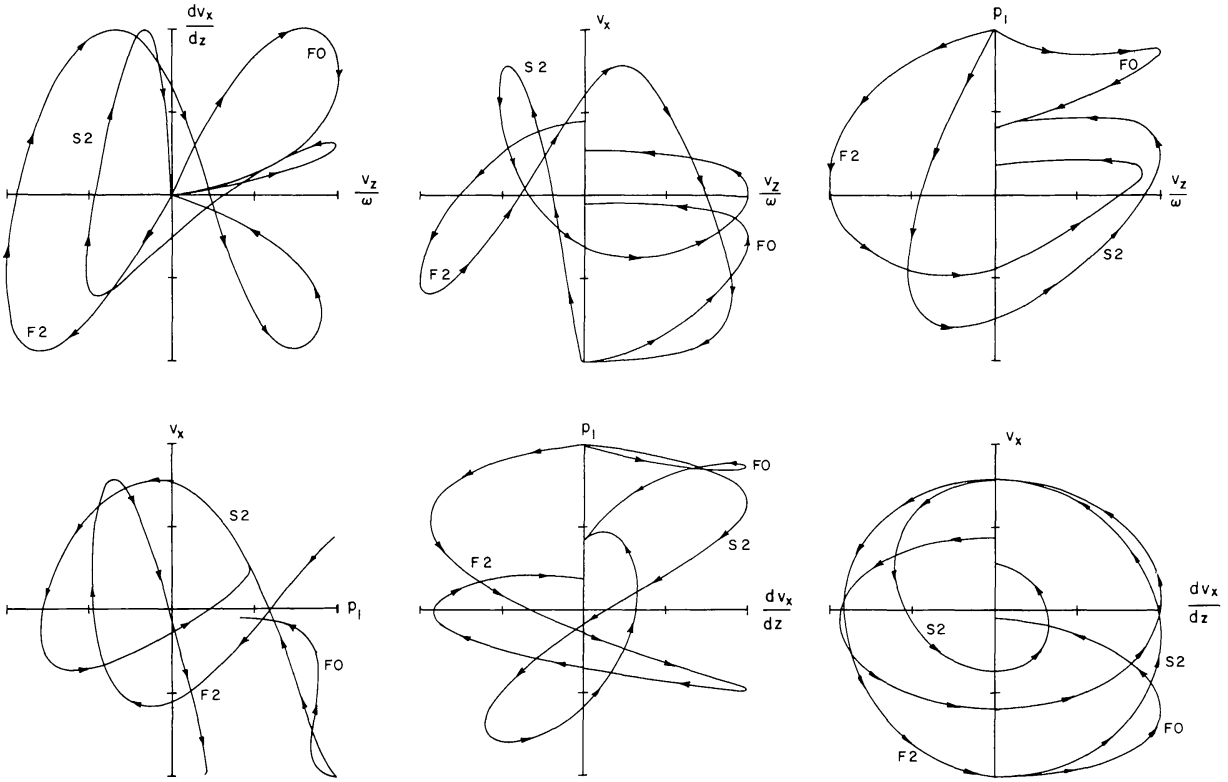

Fig. 2. The phase diagrams for $\Gamma = 1.66$, $G_B = 0.215$, $T_r = 0.33$, $\gamma = 1.1$, and $k_x = 1.0$ displaying the relative phase of all six possible pairs of the four basic perturbed quantities (v_z/ω, P_1, v_x, dv_x/dz), for three different modes (F0, F2, and S2).

v_z/ω) are out of phase and the corresponding phase paths lie essentially in the second and fourth quadrants, while for slow modes the paths lie essentially in the first and third quadrants. The F0 mode has the unique behaviour in that its phase path lies in the first or third quadrants in the $[(dv_x/dz) - (v_z/\omega)]$ plane, while it lies in the second or fourth quadrant in the $(v_x - P_1)$ plane. Such a behaviour is also observed in the phase diagrams for lower harmonics or high values of k_x. However it is found that the above phase relationship doesn't hold good for higher values of G_B and moderate values of k_x ($\simeq 1$).

(2) $[P_1 - (v_z/\omega)]$ and $[v_x - (dv_x/dz)]$ diagrams: The motion of the phase point in these diagrams is generally anticlockwise (about the origin) for both fast and slow modes, except for the F0 mode, for which the motion of the phase point is partly clockwise and partly anticlockwise. Further, normally for the successive harmonics in the same series of modes the phase point has one more node in the perturbed quantities. Thus the number of times the phase point crosses the v_z/ω (or dv_x/dz) axis in the anticlockwise sense gives the order of the harmonic involved. However, again at higher magnetic field or for a layer involving large density variation the number of crossings may not exactly give the order of harmonic involved, but still the motion of the phase point remains essentially anticlockwise in these diagrams.

(3) $[v_x - (v_z/\omega)]$ and $[P_1 - (dv_x/dz)]$ diagrams: In these diagrams the motion may appear to be quite irregular at first sight but these diagrams are the key to distinguish

between fast and slow modes. It is found that in these diagrams the motion of phase point is anticlockwise for slow modes, while it is clockwise for fast modes, thus enabling us to distinguish between the two types of modes. However again for $k_x \simeq 1$ and $G_B \geqslant 1$ the situation is somewhat complicated and the motion of phase point is in general partly clockwise and partly anticlockwise. In such cases if we count each node of eigenfunction as positive if it crosses the corresponding axis in anticlockwise sense and vice versa, then it turns out that the algebraic sum of number of nodes in these two diagrams gives a reliable and consistent index for classifying the modes. Thus if this sum is positive, we have a slow mode and for negative sum, we get a fast mode. This criterion may not always apply to the F0 mode which occupies a singular position in this respect and can be easily identified by its behaviour in $(P_1 - v_x)$ and $[(\mathrm{d}v_x/\mathrm{d}z) - (v_z/\omega)]$ diagrams.

4. Numerical Results and Discussion

We shall discuss the behaviour of growth rate with respect to various parameters of the layer for the first set of fixed boundary conditions. Table I gives the frequency (imaginary part of ω) and growth rate (real part of ω) of the various modes for $\Gamma = 1.66$, $G_B = 0.0239$, $T_r = 0.33$, $\gamma = 1.1$, and $\lambda = 3.0$ for different values of k_x and G_k. It is found that the κ-mechanism is important to overstabilize the fast modes, while the slow modes can be overstable even in the absence of κ-mechanism ($\lambda = -1$). With the increasing magnetic field the slow modes tend to be stabilized, while the fast modes are stabilized for low values of G_k, but for higher values of G_k their growth rate increases with G_B (for $G_B < 1$). Thus for low magnetic field the slow modes will dominate over the fast modes while at moderate values of magnetic field ($G_B \leqslant 1$), the fast modes begin to dominate. The growth rate of both the series of modes show a maximum with respect to the horizontal wave number k_x, as can be seen from Figure 3. This gives a preferred length scale for overstable modes. The growth rates of slow modes decrease as we go to the higher harmonics, while those of fast modes show a peak, as we go to higher harmonics. The lowest fast mode (F0) is usually stable. As in the non-magnetic case the growth rates are monotonically decreasing function of γ, and further decreasing the temperature at the top of the layer tends to destabilize the layer. For the second set of fixed boundary conditions the results are not essentially different, although in general the growth rates are somewhat lower while the frequencies are slightly higher than those for the first set of boundary conditions.

Let us consider the application of our results to the sunspot umbra. We choose the following set of parameters for the layer: base temperature of 15 000 K, base density 2.67×10^{-6} g cm^{-3} and the acceleration due to gravity $g = 2.47 \times 10^4$ cm s^{-2}. We then get a time scale of 45.21 s and length scale of 504.9 km. We take $\Gamma = 1.66$ and $T_r = 0.33$ giving a top temperature of 4950 K and layer thickness of 850.7 km. We further assume the magnetic field $B = 3000$ G ($G_B = 0.215$) and thermal diffusivity $\kappa = 2 \times 10^{12}$ cm s^{-1} ($G_k = 0.0355$), $\gamma = 1.1$ and $\lambda = 3$. Figure 3 displays the frequency

TABLE I

Real and imaginary parts of eigenvalues of the first few harmonics for $\Gamma = 1.66$, $G_B = 0.0239$, $T_r = 0.33$, $\gamma = 1.1$, and $\lambda = 3$ for different values of G_k and k_x. The numbers in parentheses are the powers of ten while the last four columns give the number of nodes in the eigenfunctions of various perturbed quantities for corresponding non dissipative ($G_k = 0$) eigenvalue.

k_x	Mode	$G_k = 0.00177$		$G_k = 0.0355$		Number of nodes in			
						v_z	P_1	v_x	$\frac{dv_x}{dz}$
0.5	S1	1.13(−3)	0.370	1.93(−2)	0.388	0	1	1	0
	F0	−9.88(−4)	0.475	−1.45(−2)	0.468	1	0	0	0
	S2	2.91(−4)	0.797	2.30(−3)	0.801	1	2	2	1
	S3	1.32(−4)	1.193	3.88(−4)	1.194	2	3	3	2
	S4	6.97(−5)	1.588	−8.31(−6)	1.589	3	3	4	3
	F1	1.30(−3)	1.643	6.71(−3)	1.666	0	1	1	1
	S5	4.83(−5)	1.983	7.26(−5)	1.984	4	5	5	4
	S6	2.99(−5)	2.378	2.50(−5)	2.379	5	6	6	5
	S7	1.90(−5)	2.774	4.89(−6)	2.774	6	6	7	6
	F2	−2.24(−3)	3.125	8.44(−3)	3.125	1	2	2	4
1.0	S1	7.95(−3)	0.296	5.03(−2)	0.374	0	1	1	0
	S2	1.19(−3)	0.784	7.75(−3)	0.798	1	2	2	1
	F0	−1.29(−3)	0.931	−1.35(−2)	0.929	0	0	0	2
	S3	5.24(−4)	1.188	1.57(−3)	1.193	2	3	3	2
	S4	2.99(−4)	1.585	3.86(−4)	1.587	3	4	4	3
	F1	7.04(−4)	1.813	8.49(−3)	1.834	0	1	1	1
	S5	2.00(−4)	1.981	3.65(−4)	1.983	4	4	5	4
	S6	1.21(−4)	2.377	1.04(−4)	2.377	5	6	6	5
	S7	7.85(−5)	2.772	2.79(−5)	2.773	6	7	7	6
	F2	−2.51(−3)	3.217	7.25(−3)	3.216	1	2	4	7
2.0	S1			9.57(−2)	0.359	0	1	1	0
	S2	5.23(−3)	0.744	2.32(−2)	0.793	1	2	2	1
	S3	2.21(−3)	1.171	5.76(−3)	1.189	2	3	3	2
	S4	1.21(−3)	1.575	1.79(−3)	1.583	3	4	4	3
	F0	−6.26(−4)	1.819	4.46(−4)	1.827	0	0	0	2
	S5	7.15(−4)	1.974	6.56(−4)	1.978	4	5	5	4
	F1	−1.46(−3)	2.371	4.61(−3)	2.387	0	1	1	2
	S6	3.81(−4)	2.373	−1.08(−3)	2.371	5	4	6	5
	S7	3.34(−4)	2.768	1.74(−4)	2.769	6	7	7	6
	S8	2.09(−4)	3.164	5.00(−5)	3.165	7	8	8	7
	F2	−3.73(−3)	3.555	9.07(−5)	3.550	1	2	2	3

and growth rate of various modes as a function of k_x. It can be seen that the maximum growth rate ($\simeq 0.04$) corresponds to S1 mode at $k_x \simeq 5$ while the fast modes have maximum growth rate of $\simeq 0.015$ for F3-mode at $k_x \simeq 2.5$. It should be noted that growth rates of slow modes decrease with G_B, while those of fast modes increase with G_B. Thus for larger values of magnetic field the fast modes are expected to dominate over the slow modes.

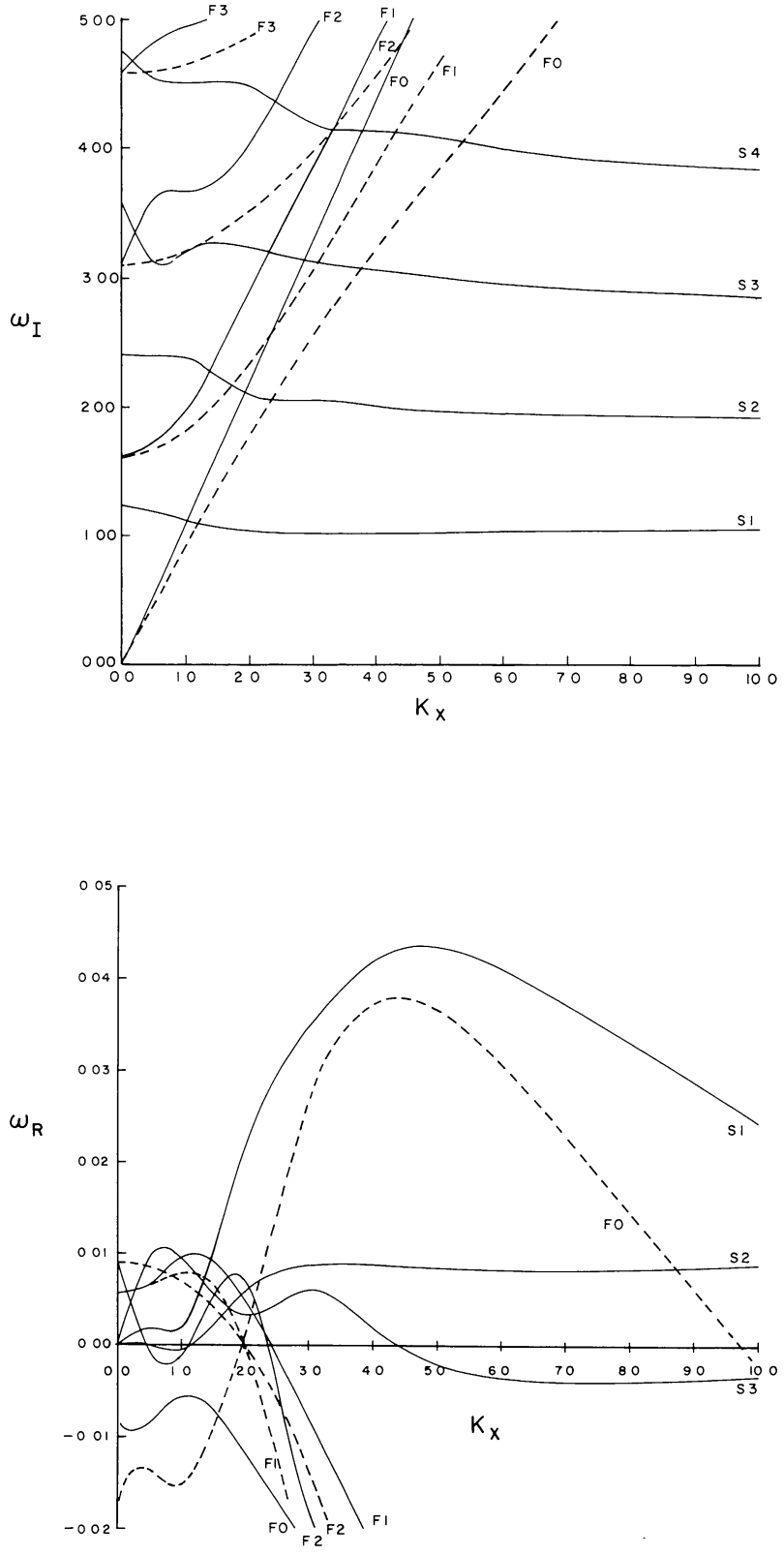

Fig. 3. Real part (growth rate, ω_R) and imaginary part (frequency, ω_I) of the eigenvalue ω are shown as a function of the horizontal wave-number k_x, for various modes for $\Gamma = 1.66$, $G_B = 0.215$, $T_r = 0.33$, $\gamma = 1.1$, $G_k = 0.0355$, and $\lambda = 3$.

All the foregoing results are obtained for fixed boundary conditions which are of course not realistic for the umbra. To approach nearer reality we have considered the free boundary conditions and it is found that the fast modes tend to be destabilized while the slow modes are slightly stabilized. Thus for the same set of parameters with the free boundary conditions, the most unstable fast mode has growth rate comparable to that of fastest growing slow mode. The approximate properties of the most unstable fast and slow modes for all the three sets of boundary conditions are summarized in Table II. These may be compared with observed periods in the range of 110–190 s and length scales of $\lesssim 1000$ km, e-folding time $\lesssim 1$ hr and phase speed $\simeq 40$ km s.$^{-1}$.

TABLE II

Most unstable modes for $\Gamma = 1.66$, $G_B = 0.215$, $G_k = 0.0355$, $T_r = 0.33$, $\gamma = 1.1$, and $\lambda = 3$

Boundary condition	Mode	Dimensionless eigenvalue	k_x	Time period (s)	Wavelength (km)	Phase speed (km s^{-1})	e-folding time (min)
I	fast	0.01+5.2i	2.5	55	1270	23	75
	slow	0.04+1.0i	5	285	635	2.2	20
II	fast	0.008+3.6i	1	80	3170	40	95
	slow	0.03+1.2i	4	235	795	3.4	25
III	fast	0.04+2.7i	1	110	3170	29	20
	slow	0.04+1.0i	4	285	795	2.8	20

5. Conclusions

The unstable modes arising in a thermally conducting compressible fluid layer in the presence of a uniform vertical magnetic field are computed. The phase relations between various perturbed quantities are examined with a view to classify the fast and slow modes. It is found that the sign of the algebraic sum of the nodes (determined by the sense of motion of the phase point) in the $[v_x - (v_z/\omega)]$ and $[P_1 - (\mathrm{d}v_x/\mathrm{d}z)]$ planes turns out to be a reliable indicator for the classification of the two series of modes.

For the range of parameters appropriate to the sunspot umbra and for free boundary conditions it turns out that the fast modes give reasonable agreement with the observed features associated with umbral flashes.

References

Antia, H. M.: 1979, *J. Comp. Phys.*, (to be published).
Antia, H. M., Chitre, S. M., and Gokhale, M. H.: 1978, *Solar Phys.* **60**, 31.
Bel, N. and Leroy, B.: 1977, *Astron. Astrophys.* **55**, 239.
Bel, N. and Mein, P.: 1971, *Astron. Astrophys.* **11**, 234.
Chandrasekhar, S.: 1961, *Hydrodynamic and Hydromagnetic Stability*, Oxford, Clarendon Press.

Chitre, S. M.: 1963, *Monthly Notices Roy. Astron. Soc.* **126**, 431.
Cowling, T. G.: 1976, *Monthly Notices Roy. Astron. Soc.* **177**, 409.
Deinzer, W.: 1965, *Astrophys. J.* **141**, 548.
Eckart, C.: 1960, *Hydrodynamics of Oceans and Atmospheres*, Pergamon Press.
Giovanelli, R. G.: 1972, *Solar Phys.* **27**, 71.
McLellan, A. and Winterberg, F.: 1968, *Solar Phys.* **4**, 401.
Moore, R. L.: 1973, *Solar Phys.* **30**, 403.
Nye, A. H. and Thomas, J. H.: 1976, *Astrophys. J.* **204**, 582.
Parker, E. N.: 1974, *Solar Phys.* **37**, 127.
Savage, B. D.: 1969, *Astrophys. J.* **156**, 707.
Scuflaire, R.: 1974, *Astron. Astrophys.* **36**, 107.
Uchida, Y. and Sakurai, T.: 1975, *Publ. Astron. Soc. Japan* **27**, 259.
Zirin, H. and Stein, A.: 1972, *Astrophys. J.* **173**, 185.